Zinc Incorporated Hydroxyapatite as Catalysts for Oxidative Desulphurization Process

M.Riad* and S Mikhail

GJRE Classification (FOR)
GJRE: C, 090402

Abstract- **Ca-hydroxyapatite was freshly prepared by precipitation method and used as a support material for preparing zinc catalysts. The catalysts were prepared by two different techniques: incipient impregnation and ionic exchange. The freshly preparedzinc catalysts were characterized via; X-ray diffraction pattern, Fourier transformer infra red spectroscopy, differential scanning calorimetery and thermo-gravimetric analyses. X-ray diffraction results established the replacement of Ca^{2+} by Zn^{2+} for the catalyst prepared by ionic exchange method and formation of Zn oxide species after impregnation. The evaluation of the catalytic activity of Zn-haydroxyapatite catalysts were investigated towards oxidative desulphurization reaction of gas oil. The results presented that desulphurization wt% was achieved to 68.5 wt% by reaction under mild conditions on using ionic exchanged zinc catalyst.**

Keywords: Hydroxyapatite, Impregnation, Ionic exchange, Zinc, Catalysts, Oxidative desulphurization.

I. INTRODUCTION

Hydroxyapatite ($Ca_{10}(PO_4)_6(OH)_2$ is widely used as bio-ceramic materials and as adsorbents for separation of bio-molecules. These materials have also been used as adsorbents for heavy metals [1], supports [2-5] and as catalysts in oxidation and dehydrogenation reactions. The catalytic performance of these materials depend on the lattice substitution of Ca sites in hydroxyapatite structure by varied cations as Na, Mg, Sr and Mn, which result in changes in various structural properties as crystallinity and morphology. The preparation of hydroxyapatite with controlled morphology, stoichiometery, crystallinity and size has the main role in production of an active catalytic material. Various synthesis methods have been used for hydroxyapatite preparation such as, soild state reaction [6], chemical precipitation [7], formation of hydroxyapatite crystals on glass or brushite growth of hydroxyapatite crystal using sol gel synthesis and surfactant tamplating method.Hanna and Hamid [8] studied the preparation of Ca-hydroxyapatite via electro-deposition method of highly pure brushite ($CaHPO_4.2H_2O$) on titanium alloy substrate and the transformation of brushite to hydroxyapatite as a coating for orthopaedic implants. Filho et al, [9] investigate the preparation of Fe-hydroxyapatite by high energy dry milling of calcium nitrate and ammonium phosphate with different amounts of iron oxide (0.5, 1 , 2.5 and 5wt%) and calcined at 900°C. Cd-hydroxyapatite were synthesized by high temperature mixing method using solution of $Cd(NO_3)_2.4H_2O$ and $(NH_4)_2HPO_4$ at different pH values: 10 14 and found the pH values have a great influence on the crystallinity and morphology of hydroxyapatite [10].

Akuma et al, [11] study the preparation of Ag-loaded hydroxyapatite by incipient impregnation technique using different silver loading of $AgNO_3$ (0.5, 1, 1.5 and 2 wt%). Fe- [12] and V- substitute hydroxyapatite [13] were prepared by co-precipitation technique. Zn -substituted hydroxyapatite prepared by ionic exchange technique was an efficient catalyst for the synthesis of 3-substituted indoles [14].The aim of this work is to prepare Ca-hydroxyapatite by precipitation technique to be used as a support material. The effect of incorporation of Zn^{2+} ions either by impregnation and or ionic exchange techniques with different zinc loading on the crystallinity, crystallite size, formed phases and thermal stability of all prepared materials were investigated. The catalytic activity of the prepared Zn-hydroxyapatite catalysts towards oxidative desulphurization of gas oil was also studied

II. EXPEIMENTAL

1. *Preparation Of The Support Materials*

Hydroxyapatite (Hap) was prepared by co-precipitation technique according to Narasaraju et al, [15] and Tkalcec et al, [16] methods. A 0.3 M $(NH_4)_2HPO_4$ solution was drop wisely added to 0.5 M $Ca(NO_3)_2$ solution and the pH was adjusted to 11 by adding ammonia solution until a white suspension was obtained. The suspension was further stirred for 24 hours, then filtered and washed with distilled water. The resultant cake dried at 100°C and then calcined at 400°C in presence of flow of purified air.

2. *Preparation Of Zn-Hydroxyapatite Catalysts*

a) *Wet Impregnation Technique*

10 and 20wt % Zn/hydroxyapatite catalysts (based on the weight of support) were prepared by wet impregnation technique using zinc nitrate as a salt solution. The prepared catalysts ($ZnHap_{Imp1}$ and $ZnHap_{Imp2}$) dried at 120°C and then calcined at 350°C for 3 hours.

b) *Ionic Exchange Technique*

A 0.1 and 0.2 M solutions of $Zn(NO_3)_2.H_2O$ were kept in contact with 10gm of the prepared hydroxyapatite material for 48 h under agitation at room temperature to prepare $ZnHap_{Ion1}$ and $ZnHap_{Ion2}$ catalysts. The resultant cake was filtered, dried at 100°C for 24 h and then calcined at 350°C for 3h.

3. *Characterization*

X –ray Diffraction Pattern (XRD) was carried out on XD-D1- x-ray diffraction Schimadzu, CuKα radiation was the light source

About-Egyptian Petroleum Research InstituteNasr City, Hai Al-Zehour PO Box 11727, Cairo, Egypt

with applied voltage of 40K and current of 40 mA. Two theta angles ranged from 4 to 80° with speed of 2° per minute, the formed phases of the prepared and calcined materials were detected. The crystallite size was calculated from X-ray line broadening using Sherrer's equation $D= k\lambda /\beta_{1/2}\cos\theta$, where D is crystallite size estimated using the reflection (002), k is a shape factor equal 0.9, λ is X-ray wave length (CuK_α =1.5405), θ is the diffraction angle related to reflection 002 (θ = 25.86), and $\beta_{1/2}$ calculated using the formula $\beta_{1/2}= (B^2-b^2)^{1/2}$, where B being the diffraction peak width at half height and b is the natural width of the instrument [17].The crystallinity degree (Xc) corresponding to the fraction of crystalline phase present in examined volume was evaluated according to Landi et al., [18]. $Xc \approx 1- (V_{112-300}/I_{300})I_{300}$ is the intensity of (300) reflection of apatite and $V_{112-300}$ is the intensity of the hollow between (112) and (300) reflection.The values of lattice parameter were determined from characteristics diffraction pattern using the Retiveld full profile method and Koalarie computer software [19,20]. In addition, the volume of unit cell is calculated using lattice parameter of hydroxyl-apatite a/c by the formula : $V=2.589a^2c$ Fourier Transformer Infra Red (FT-IR) spectra were run on Perkin Elmer FT-IR apparatus working in the range of 4000-400 cm^{-1} to identify the hydroxyl and functional groups contained the prepared and calcined materials.Differential Scanning Calorimetry Analysis (DSC) was carried out using the Differential Thermal Analyzer, Perken Elmer apparatus, to study the phases formed upon thermal treatment and the enthalpy of prepared catalysts.The Ca/P ratio and the metal loading was determined by X-ray flourcence (XRF) using Rigaku Seqential Spectrometer (RIx3100) equipment with Rh source

4. Catalytic Reaction

The catalytic oxidative desulphurization reaction of gas oil (supplied from Cairo Refining Petroleum Company) was carried out in a triple-necked round bottomed flask at reaction temperature 60°C in the presence of the different prepared zinc catalysts and using hydrogen peroxide as oxidizing reagent. For each, 50 ml of gas oil and 50ml of hydrogen peroxide (30%water, Prolabo) was added to 1 gm freshly prepared catalyst. The reaction mixture was stirred for 1 hour and settled to attain phase separation. Then, the separated gas oil was adsorbed on activated bentonitec-clay material at 50°C. The sulphur concentration was measured by X-ray flourcence apparatus (Horiba SFLA-1800).

III. Results and Discussions

The chemical composition of support and the prepared catalysts was obtained by XRF and the results are tabulated in Table 1). The measured Ca/P atomic ratio is 1.67 which is coincident with that for the stoichiometric hydroxyapatite material.

1. Catalysts Characterization

a) X-Ray Diffraction Pattern

Fig.1 shows X-ray diffraction patterns for hydroxyapatite and the prepared zinc catalysts. The diffraction lines appeared at 2θ = 25.8, 29.1, 31.9, 33.1, 32.2, 34.1, 40.1, 46.9, 49.1° (Fig.1a) attributed to the presence of crystalline hydroxyapatite phase $Ca_5(PO_4)_3(OH)$ {ASTM 76-0694}.The diffracto-gram for calcined hydroxy-apatite (Fig.1b) ascribed a well crystalline structure as established from the increase in the crystallinity degree from 35 to 45% (Table2) and the appearance of sharp diffraction lines with high intensities, in comparing to as-prepared one. The diffraction pattern for $ZnHap_{Imp1}$ catalyst (Fig.1c) reflects a decrease in line's intensities which ensure an incorporation of Zn cation in the hydroxyapatite lattice structure. Further increase of Zn loading the intensity of the hydroxyapatite lines are also decreased. Upon calcination of $ZnHap_{Imp1}$ the diffraction lines became sharp and the crystallinity degree increases from 45% then to 55 and 63% with the increase in Zn content up to 20 wt% (Fig. 1e & Table 2), in agreement with Suchanek et al, [21] and Feng et al, [22] investigations. In addition, new diffraction lines appeared at 2θ =32.0, 37.2, 49.5° emphasized the presence of ZnO species (Fig. 1f). For $ZnHap_{Ion1}$ catalyst no visible changes are observed in the diffraction lines (Fig.1g). Meanwhile, XRD pattern for $ZnHap_{Ion2}$ catalyst reveals a shift in the hydroxyapatite diffraction lines to higher angles which indicated that Ca^{2+} cations were substituted by Zn ones in the hydroxyapatite structure (Fig. 1h). At the same time, the diffraction lines are broadened owing to the low crystallinity of Zn replaced hydroxyapatite compared to the support material, in accordance with Wakamura et al, [23] proposal that divalent ions difficult to obtain high crystallinity and greatly inhibit hydroxyapatite crystallization.On the other hand, parascholzite phase $CaZn_2(PO_4)_2.2H_2O$ appeared at 2θ = 10, 12.5, 20° (ASTM 76-0725) upon calcination of. $ZnHap_{Ion2}$ catalyst, in agreement with the results of Mujaji et al, [24] who reported that the formation of Zn substituted hydroxyapatite by precipitation technique and the formation of parascholzite phase started to form at Zn fraction up to 18 wt% and estimated a limit of 15 mole % for Zn substitution in Hap lattice.

b) Crystallite Size

The average crystallite size for the prepared materials was determined using Sherrer's equation at 2θ = 25.86° (002) plane. The results in Table 2 reveal an increase in crystallite size from 16.0 to 21.6 nm for the calcined hydroxyapatite one due to the removal of the hydroxyl groups upon heating, which allow the aggregation of the particles, in accordance with the sharpness of diffraction lines and the increase in the crystallinity degree. For $ZnHap_{Imp1,2}$ catalysts, the crystallite size shows an increase that may be resulted from the aggregation of ZnO species within apatite lattice. On contrary, the crystallite size for $ZnHap_{Ion}$ decreases with the increase of the replaced Zn cations up to 20%.

c) Lattice Parameter

Diffracto-gram analysis allowed the identifications of the hexagonal phase with lattice parameter of hydroxyapatite which augmented gradually from 0.9425 to 0.9462 nm (for a=b) and from 0.6906 to 0.648 nm (for c) with the increase of zinc loading (impregnation method) from 10 to 20 wt% respectively, in agreement with Parhi et al investigations [25]. Where the expansion of lattice parameter was consistent with the incorporation of Zn^{2+} into Ca^{2+}-hydroxyapatite lattice. For $ZnHap_{Ion}$ catalysts, both a and c decrease with the increase in the Zn substituted catalysts. Whereas, a=b shows a further decease upon heating and c shows the reverse (Table 2). As well known that the divalent cations like Zn causes a lattice strain upon heating, and consequently the lattice structure of Ca-hydroxyapatite was disordered, in accordance with the results of unit cell volume which contracts and relaxes as the lattice parameter either decrease and or increase (Table 2).

d) Thermal Behavior

Fig. 2 represented differential scanning calorimetery (DSC) and thermogravimetric (TG) profiles for the prepared hydroxyapatite and Zn-hydroxyapatite catalysts and the calculated enthalpy and weight loss% included in Table 3.DSC profile for hydroxyapatite reveals the appearance of an endothermic peak in the range of 30-120^{o}C attributed to the desorption of water adsorbed on the crystallite surface of hydroxyapatite and a second endothermic peak appeared at 860-930 ^{o}C which related to decomposition of hydroxyapatite structure. From literature, hydroxyapatite is stable at higher temperature and decompose to the β-tricalcium phosphate at temperature higher than 1350 ^{o}C above this temperature β- irreversibly transform to α- form [8]. Tkalcec et al, [16] established that hydroxyapatite prepared by precipitation start to decompose at 800^{o}C when heated and transforms to tri-calcium phosphate.For $ZnHap_{Imp1}$ catalyst the DSC profile shows the same behavior as hydroxyapatite material. Further increase in Zn loading to 20w%, a new endothermic peak appeared at 250 -300^{o}C which imply the formation of ZnO species. On the other hand, the heat of enthalpy for the endothermic peak appeared at 860-930^{o}C (Table 3) increased with increasing the zinc loading [26] which means the more restrained hydroxyapatite structure.DSC profile for $ZnHap_{Ion1}$ catalyst is also similar to that for the support with an observed increase in heat of enthalpy related to the incorporation of Zn species in the support lattice (Table 3). For $ZnHap_{Ion2}$ catalyst DSC profile reveals the appearance of two endothermic peaks in addition to the surface adsorbed peak at 30-160^{o}C. The peak appeared at 480-620^{o}C related to the removal of lattice water, in accordance with Le Geros et al, [27] who reported that Ca deficient hydroxyapatite incorporate water which substitute for OH sites and called lattice water that vaporized gradually at 140-600^{o}C. The endothermic peak that appeared at 650-820^{o}C is ascribed to the transformation of hydroxyapatite to tri-calcium phosphate which means Zn might promote this transformation process. Moreover, an exothermic peak appeared at 220-320^{o}C which imply the dehydroxylation of hydroxyapatite structure and the formation of paraschlozite phase.

Thermo-gravimetric line for the prepared hydroxyapatite (Fig. 2) exhibits two steps for weight loss, the first at 30-120^{o}C due to the desorption of water adsorbed on the surface of apatite particles and the second at 860-930^{o}C due to the transformation of hydroxyapatite to tri-calcium phosphate. It is noticed that, the weight losses increase with increasing Zn content.

e) Ft-Ir Spectroscopy

Fig. 3 shows FT-IR spectra for Hap and zinc catalysts recorded at wave number ranged from 4000 to 400 cm^{-1}.FT-IR spectrum for hydroxyapatite in Fig. 3a reveals the appearance of phosphate (PO_4^{-3}) bands which attested by the P-O asymmetric and symmetric stretching mode appeared at 965, 1030, 1095 cm^{-1} and the O-P-O bending modes at 605, 565, 475 cm^{-1}. Adsorbed molecular water band appeared at 1630 cm^{-1} and also a shoulder at 875cm^{-1} assigned to $(HPO_4)^{-2}$ which formed upon the reaction of some surface PO_4^{-3} with water. Two bands appeared at 630 & 3580 cm^{-1} assigned to vibrational and stretching modes of OH groups respectively. After heat treatment, Fig.3b reveals that the broad band appeared at ~3400 cm^{-1} became smaller which related to the decrease in the amount of lattice and adsorbed water. Tanaka et al, [28] found that the number of surface P-OH decreased by 60% on heating to 600^{o}C resulting in the formation of P-O-P group as 2P-OH = P-O-P +H_2O. Loading of Zn on hydroxyapatite leads to increase in the band intensity appeared at 1630 cm^{-1}. With the increase in Zn loading the spectrum in Fig. 3c,d clarified the intensities of stretching bands (associated with phosphate bands) at 965, 1030, 1095 cm^{-1} reduced and the resolution of such bands became obscure and the OH bending band at 630 cm^{-1} was broadened owing to the decrease in the crystallinity of the prepared material, in agreement with XRD results. For calcined Zn catalysts the profile in Fig. 3 shows a decrease in the intensity of the band at 3580 cm^{-1} assigned to stretching vibration of structural OH group located on hydroxyapatite tunnels. The decrease in peaks intensity may be ascribed to the dehydroxylation that accompanied the calcination step and the formation of other species. In addition, band appeared at 2150 cm^{-1} assigned to the formation of ZnO species (for $ZnHap_{Imp2}$ catalyst, Fig. 3h), whereas, band appeared at 2200 cm^{-1} assigned to the formation of paraschlozite phase (for calcined $ZnHap_{Ion2}$ catalyst, Fig. 3j).

2. Catalytic Evaluation

The activity of support and the prepared catalysts was evaluated towards oxidative desulphurization reaction of light gas oil containing 1281.8 ppmw sulphur. As previously investigated [29], sulphur compounds containing light gas oil consist mostly of benzothiophene and dibenzothiophene derivatives. Experimentally, gas oil was mixed with hydrogen peroxide as oxidizing reagent (1:1 vol ratio) at 60^{o}C with vigorous stirring for one hour. The formed sulphons was removed via adsorption on activated

bentonitec clay materials. The results are included in Table 4. From data, it is clear that, the sulphur content decreased from 1281.8 (Feed) to 930.5 ppm on using the prepared hydoxyapatite material i.e. desulphurization wt% reached to ~27wt%. The results in Table 4 revealed that the prepared catalysts exhibits remarkably high activities in the removal of sulphur compounds by mild oxidation with hydrogen peroxide compared with support material. The sulphur content decreases to 490.7 ppmw on using $ZnHap_{Imp1}$ catalyst. Whereas, on increasing zinc loading from 10 to 20 wt%, the removal of sulphur does not affected.On the other hand, the content of sulphur deceases from 1281.2 (Feed) to 512.9 ppmw using $ZnHap_{Ion1}$ catalyst, further increase in the replaced Zn cations, the removal shows a sharp increase (Table 4).As shown in Table 4 $ZnHap_{Ion2}$ has the highest activity in sulphur removal reaches to 877.6 ppmw (desulphurization 68.5 wt%) after 60 min of reaction. These results are in agreement with that studied by Ishihara et al, [30] who reported that the removal of sulphur in light gas oil from 39 to 5 ppmw (~88%) by an oxidation –adsorption continuous flow process. Also, it decreased from 320 to 10 ppmw in diesel fuel fraction on using Mo/Al_2O_3 catalysts [31]. Moreover, Venugopal et al, [32] and Venugopal et al, [33] studied the oxidative desulphurization reaction of light petroleum fractions on titanium containing molecular sieve and gold supported on hydroxyapatite, where the sulphur removal reached to 56% and 80% respectively under the same experimental conditions. These established that the preparation of hydroxyapatite material to be used as support to prepare Zn catalysts for oxidative desulphurization reaction. of gas oil. Thus, the sulphur removal data emphasizes that $ZnHap_{Ion2}$ is the most active catalyst towards oxidative desulphurization process where the sulphur removal reaches 68.5wt%.

3. Mechanism Of Reaction

According to Basolo et al, [34] active species of Zn oxide can be formed by the nucleophilic attack of hydrogen peroxide on Zn atoms, electrons are withdrawn from the peroxyl moiety, thereby increasing the electrophilic characters of the peroxidic oxygen. The oxidation of sulphur atom in the organo-sulphur compound must proceed by nuclophilic attack of an active hydroperoxy to form sulphoxide and a regenerated zinc species. Subsequently, the sulphoxide undergoes further oxidation by hydroperoxy to form sulphone, it is possible to rationalize the presence of electronegative phosphate species as they help withdraw electrons density from Zn species and thereby conferring a higher electrophilic character to the Zn, in agreement with the mechanism proposed by Ramirez et al, [31] . Hydrogen peroxide migrates to Zn sites with an OH to form an intergradations of hydroperoxide species responsible for oxidation of sulphur compound, sulphur substrates possibly going through two steps pathways are oxidized into sulphoxide or sulphone. Concurrently, the formed paraschllozite phase in calcined Zn (20wt%) exchanged apatite catalyst offers the required species for oxidative desulphurization mechanism of light gas oil.

IV. Conclusion

- The hydroxyapatite material was prepared by precipitation method, 10 & 20wt% zinc-hydroxyapatite catalysts were prepared via either impregnation and or ionic exchange techniques.
- The different preparation techniques used were suitable to incorporate zinc phase and the catalyst presented significant differences in relation to the formed phase
- For zinc catalyst loaded hydroxyapatite, Zn was incorporated as ZnO species (after calcinations) as confirmed from X-ray diffraction analysis.
- For zinc replaced hydroxyapatite Zn was incorporated into apatite lattice.
- Zinc replaced catalyst has high activity towards the oxidative dehydrogenation reaction of gas oil under mild conditions.

V. References

1) M. Miyake, K. Watanabe, Y. Nagayama, H. Nagasawa, T. Suzuki, J. Chem. Soc. Faraday Trans. 86 (1990) 2303.
2) AVenugopal, M.S. Scurell, Appl. Catal. 245 (2003) 137.
3) Z. Opre, J.D. Grunwaldt, M. Maciejewski, D. Ferri, T. Mallat, A. Baiker, J. Catal. 230 (2005) 406.
4) N.S. Resende, M. Nele, V. M. Salim, Thermochim Acta 451 (2006) 16.
5) G. Lopez, R. Pomes, C.O. Vedova, R. Vina, J. Raman Spectrosc. 32 (2001) 255.
6) S. Sugiyama, T. Shona, D. Makino, T. Moriga, H. Hayashi, J. Catal. 214 (2003) 8.
7) K. Elkabouss, M. Kacimi, M. Ziyad, S. Ammar , F. Bozon-Verduraz, J. Catal. 226 (2004) 16.
8) F. Hanna, Z. Hamid, Pigment and resine technology, 5 (2003)19
9) F.P.Filho, R.E.F.Q. Nogueira, M.P.F. Graca, M.A. Valentie, A.S.B. Sombra, C.C.Silva, Physica B, 403 (2008)3826-3829.
10) K.Zhu, K. Yangiswa, A. Onda, K. Kajiyoshi, J. Qiu, Materials Chemistry and Physics, 113 (2009) 239.
11) P.Akumar, M.P. Reddy, L.K. Ju, H. H. Phil, Catal Lett., 49 (2008)31.
12) W. Pon-on, S. Meejoo, I-M. Tang, Materials Research Bulletin , 43 (2008) 2137.
13) S.Sing, S.B. Jonnalagaddo, Catal. Lett., 49 (2008) 45.
14) R. Tahir, K. Banest, A. Solhy, S. Sebti, J. Mol. Catal. 246(2006)39.
15)] T.S.B. Narasaraju, D.E. Phebe, J. Mater. Sci., 31 (1996) 1.
16) E. Tkalcec, M. Sauer, R. Nonninger, H. Schmidt, J. Mater . Sci. 361 (2001) 5233.
17) T. J. Burgues, R.R. Clemente, Cryst. Res. Technol. 36 (2001) 1075.
18) E. Landi, A. Tampier, G. Celotti, S. Spria, J. Eur. Ceram. Soc. 20(2002)2377.

19) H. Rietveld, J. App. Cryst. 2 (1969)65
20) R.W. Cheary, A. A. Coechlo, J. App. Cryst. 25(1992) 109
21) W.L.Suchanek, K. Byrappa, P. Shuk, R.E. Riman, V.F. Janas, K.S. Ten-Huisien, Biomaterials, 25(2004) 2647
22) Z.D. Feng , Y.M. Liao, M. ye, J.Mater. Sci. Mater. Med. 16(2005) 417.
23) M. Wakamura, K. Kandori, T. Ishikawa, Colliod and Surf. A. 164 (2000) 297
24) F. Mujaji, Y. Kono, Y. Suyama, Materials Research Bulletin. 40 (2005)209.
25) P. Parhi, A. Ramanan, A.R. Ray, J. Mater. Sci, 41(2006)1455.
26) T.M. Sridhar, U.K. Mudali, M. Subbaiyan Corr. Sci. , 45 (2003) 2337.
27) G. Z. Le Geros, C. B.Bleiwas, M. Retino, R. Rohanizadeh, I.P. Le Geros, Am. J. Dent. 12 (1999) 65.
28) H.Tanaka, M. Chikazawa, K. Kandori, T. Ishikawa, Phys. Chem. Chem. Phys. 2 (2000) 2647.
29) J. L. Garcia-Gutierrez, G. A. Fuentes, M. E. Hamandez-Teran, F. Murrieta, J. Navarrete, F. Jimenez-Cruz, Appl. Catal. A. 305 (2006) 15.
30) A. Ishihara, D. Wang, F. Dameignil, H. Amano, E. W. Quiam, T. Kabe, Appl. Catal. A 275 (2005) 279.
31) L.F. Ramirez, E. Torres, R. Gomez, V. Gonzalez, F. Murrieta, Catal. Today, 98 (2004) 289.
32) V. Hulea, F. Fajula, J. Bousquet, J. Catal. 198 (2001) 179.
33) A. Venugopal, M. S. Scurrecll, Appl. Catal. A 245 ((2003) 137.
34) F. Basolo, R. G. Pearson, Mechanism of Inorganic Reaction , Second ed., Wiley, NewYork,1962.

Table (1): Chemical Composition of the Prepared Hydroxy-apatite and Zinc Catalysts

Catalysts	Calcium wt%	Phosphorus wt%	Ca/P ratio
Hap	35.67	16.54	1.67
$ZnHap_{Imp1}$	35.88	16.53	1.70
$ZnHap_{Imp2}$	35.78	16.54	1.69
$ZnHap_{Ion1}$	34.56	16.51	1.57
$ZnHap_{Ion2}$	34.49	16.51	1.56

Table (2): Lattice Parameters, Crystallite Size and Degree of Crystallinity for Hydroxy-apatite and Zinc Catalysts

Catalysts	a=b (nm)	c (nm)	Volume of unit cell (nm^3)	Crystallite Size (nm)	Degree of Crystallinity(%)
Hap	0.9425	0.6881	0.5311	16.0	35
Calcined Hap	0.9441	0.6906	0.5330	21.6	45
$ZnHap_{Im1}$	0.9450	0.6873	0.5292	28.7	39
Calcined $ZnHap_{Im1}$	0.9442	0.6858	0.5290	30.4	55
$ZnHap_{Im2}$	0.9453	0.6860	0.5277	35.5	33
Calcined $ZnHap_{Im2}$	0.9438	0.6843	0.5271	44.8	63
$ZnHap_{Ion1}$	0.9420	0.6876	0.5308	20.9	28
Calcined $ZnHap_{Ion1}$	0.9416	0.6882	0.5306	19.3	21
$ZnHap_{Ion2}$	0.9418	0.6873	0.5305	14.5	22
	0.9415	0.6870	0.5302	10.2	18

Table (3): Thermal Behavior Data for Hydroxy-apatite and Zinc Catalysts

Catalysts	Peaks Location (^{o}C)	Enthalpy(Cal/gm.sec.)	Weight Loss%
Hap	30-120 (endo) 860-930 (endo)	17.71 14.3	4.34 10.47
$ZnHap_{Im1}$	35-125 (endo) 850-930 (endo)	27.3 18.6	10.45 12.82
Zn Hap_{Im2}	30-100 (endo) 250-300 (endo) 860-920 (endo)	37.99 19.65 23.52	16.53 17.71 19.66
Zn Hap_{Ion1}	25-100 (endo) 850-930 (endo)	8.65 27.8	7.59 21.6
Zn Hap_{Ion2}	30-160 (endo) 220-320 (exo) 480-620 (endo) 650-820 (endo)	17.74 16.35 24.85 39.57	11.24 5.97 12.16 29.45

Table (4): Oxidative Desulphurization Results of Light Gas Oil on the Prepared Zinc Catalysts

Catalyst	Feed	Hap	ZnHapIm1	ZnHapIm2	ZnHapIon1	ZnHapIon2
Sulphur Content ppm	1281.2	930.5	490.7	612.8	512.9	403.6
Sulphur removal ppm	0	350.3	790.5	668.4	768.3	877.6
Desulphurization,wt%	0	27.3	63.4	52.2	60.0	68.5

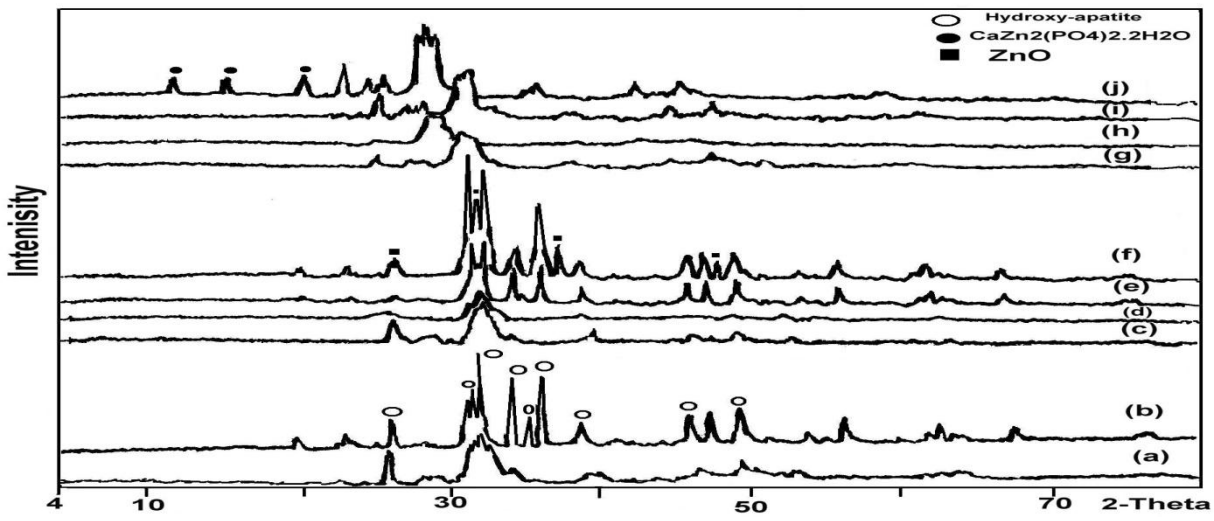

Fig. (1): XRD Spectrum for: (a) Hap (b) Calcined Hap (c) Prepared $ZnHap_{Im1}$ (d)Prepared Zn Hap_{Im2} (e) Calcined $ZnHap_{Im1}$ (f)Calcined $ZnHap_{Im2}$ (g) Prepared $ZnHap_{Ion1}$ (h) Prepared Zn Hap_{Ion2} (i) Calcined Zn Hap_{Ion1} (j) Calcined Zn Hap_{Ion2}

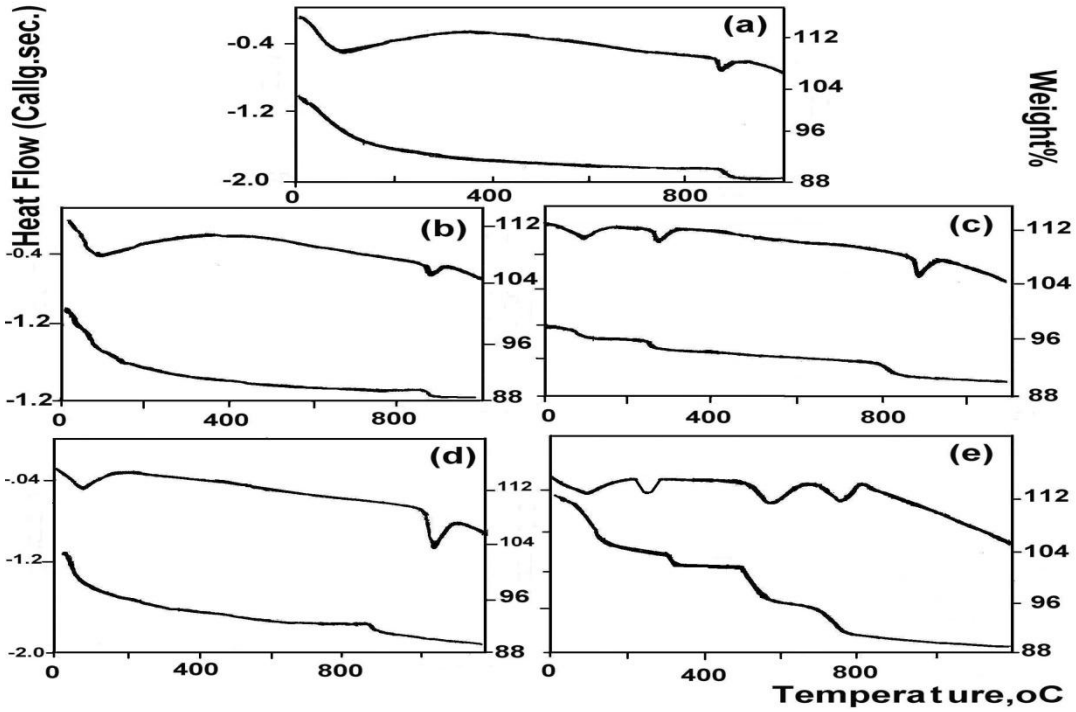

Fig. (**2**): Differential Scanning Calorimetery Profile for:
(a) Hap (b) Prepared $ZnHap_{Im1}$ (c) Prepared Zn Hap_{Im2}
(d) Prepared $ZnHap_{Ion1}$ (e) Prepared Zn Hap_{Ion2}

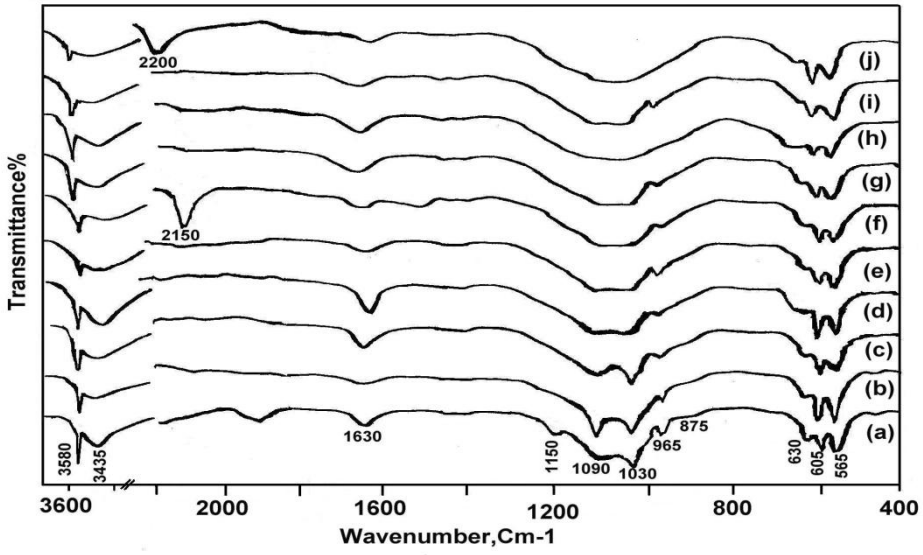

Fig. (3): FT-IR Spectrum for: (a) Hap (b) Calcined Hap (c) Prepared $ZnHap_{Im1}$ (d) Calcined $ZnHap_{Im1}$ (e) Prepared Zn Hap_{Im2} (f)Calcined $ZnHap_{Im2}$ (g) Prepared $ZnHap_{Ion1}$ (h) Calcined Zn Hap_{Ion1} (i) Prepared Zn Hap_{Ion2} (j) Calcined Zn Hap_{Ion2}